07

Functional transformation of random signals in a composite magnetoelectric cell

 L.M. Krutyansky, V.L. Preobrazhensky

Prokhorov Institute of General Physics, Russian Academy of Sciences, Moscow, Russia
E-mail: leonid.krut@kapella.gpi.ru

Received February 13, 2025
Revised March 11, 2025
Accepted March 17, 2025

Results of calculations of transfer functions for a composite magnetoelectric cell exposed by random sequences of pulsed signals are reported. Threshold conditions are found for generation of single spikes and random sequences of pulses with fixed amplitude using a combined numerical-analytical method. Probability of switching between the states of the magnetic system is controlled by the magnetization field. Effects of accumulation and threshold-type change of state with switching of polarization like „Integrate-and-fire"behavior are demonstrated for unipolar and bipolar sequences of random input signals. It is shown that in the case of bipolar input signals a steady generation of a stochastic spike sequence is obtained with a random delay of the magnetic subsystem in stable states. The results are aimed at applications in the domain of development of stochastic neuromorphic systems.

Keywords: functional magnetoelectric transformer, random signals, stochastic spikes, excitation threshold, accumulation and switch effect.

DOI: 10.61011/TPL.2025.06.61294.20282

The progress in development of artificial intelligence systems stimulates the interest in analog elements of neuromorphic networks that perform certain functional transformations of signals. Transformations imitating the functions of neurons include weighted summation of input signals from different network elements, nonlinear transformation of the sum, and formation of an output signal that acts as an activation function [1]. In neuromorphic networks operating with pulse sequences (spiking neural networks, SNNs), an artificial neuron produces a single pulse (spike), which is transmitted to the network, under certain threshold conditions at the input. When processing pulse signals, a neuron may perform the function of accumulation of information with a threshold state change (integrate-and-fire) and subsequent relaxation. Various semiconductor, ferroelectric, photonic, spintronic, phase-transition, and electrochemical physical implementations of artificial neurons were discussed in review [2]. A straintronic functional signal converter in the form of a magnetoelectric composite in the region of a spin-reorientation transition, which performs summing of signals from a multichannel input, forms a nonlinear activation function and a threshold spike response, and exhibits the integrate-and-fire effect of accumulation and resetting of the potential, was proposed in [3]. Various functions of nonlinear signal transformation are implemented in this case within a single structure by controlling the parameters of the magnetization field and input signals.

In stochastic SNNs operating with random pulse signals, stochasticity may be incorporated either into the time sequence of pulses of a fixed amplitude [4–9] or into the amplitude of pulses of an equidistant sequence [10]. In the present study, the functional characteristics of a straintronic converter processing a sequence of pulse input signals of a random amplitude are investigated using a combined numerical and analytical modeling method. Magnetic field-controlled threshold conditions for the generation of random spike pulse sequences with a fixed amplitude are determined.

The simplified diagram of a straintronic magnetoelectric converter is shown in Fig. 1, *a*. Layers of magnetic metal with a total thickness of $150\,\mu$m are deposited onto both sides of a piezoelectric plate $4 \times 4 \times 0.3$ mm in size. In addition to contributing to magnetoelectric coupling, these layers act as output and ground electrodes. The input and output electrodes are separated by a dielectric layer (TiO_2) with a thickness of $5\,\mu$m. The electrodes are connected via leakage (or load) resistances. Ferroelectric PMN−PT ($\langle 011 \rangle$ cut) is used as a piezoelectric material [11], and layered $TbCo_2$/FeCo nanostructures with giant magnetostriction serve as a magnetic metal [12–14]. It is assumed that uniaxial magnetic anisotropy is induced in the magnetic layers in the process of deposition. Figure 1, *b* shows the relative orientation of the easy magnetization axis (EA), the crystallographic axes of the piezoelectric, and the vectors of magnetization and the control magnetic field. Magnetoelectric coupling is established due to the joint deformation of the piezoelectric and magnetic layers. The calculation performed numerically in the COMSOL Multiphysics package specified the dependence of quasi-static deformations averaged over the magnetic volume on voltage V_{out} across the piezoelectric and magnetization orientation angle φ [3]:

$$\langle u_{xx} - u_{yy} \rangle = g_p V_{out} + g_m^{(1)} \sin 2\varphi,$$
$$\langle u_{xy} \rangle = g_m^{(2)} \cos 2\varphi, \qquad (1)$$

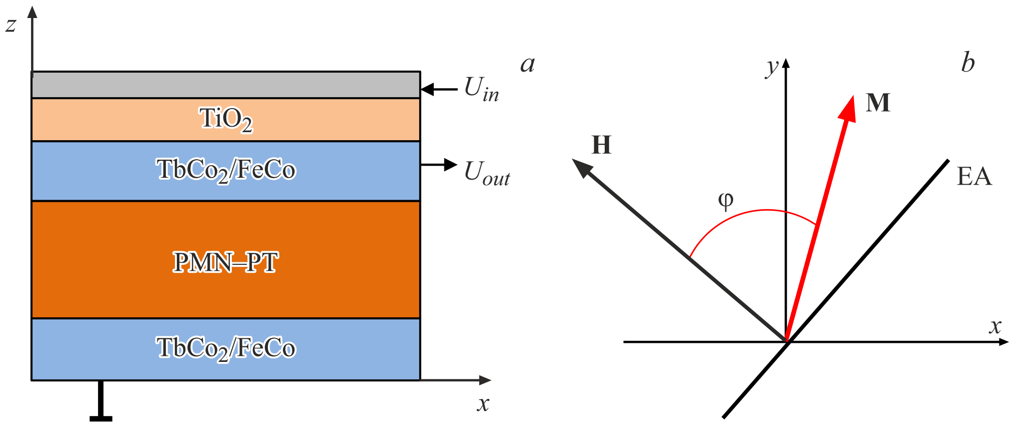

Figure 1. Schematic diagram of a composite magnetoelectric cell (*a*) and diagram of mutual orientation of the vectors of magnetization **M** and magnetization field **H** and easy magnetization axis EA (*b*). The input electrode is at the top.

where

$$g_p = -0.07 \cdot 10^{-5}\,\mathrm{V}^{-1},$$

$$g_m^{(1)} = -10^{-4},\, g_m^{(2)} = -3.1 \cdot 10^{-5}$$

— result of numerical calculations.

The dynamics of slow (compared to the spin relaxation time) processes is characterized by a coupled system of the equation of state of the magnetic system and the equation of relaxation of normalized charge P at the piezoelectric plate [3]:

$$\frac{H}{H_A}\sin\varphi - \frac{1}{2}\sin 2\varphi = \left[P + U_{in} - (\kappa+\eta)\sin 2\varphi\right]\cos 2\varphi, \tag{2}$$

$$\frac{\partial P}{\partial t} = -\frac{1}{\tau}(P - \kappa \sin 2\varphi) - U_{in}\left(\frac{1}{\tau} - \frac{1}{\tau_1}\right), \tag{3}$$

where dimensionless variable $U_{in} = 2V_{in}g_p \cdot 0.78B/MH_A$, B — magnetoelastic interaction constant (on the order of -10 MPa for $TbCo_2$/FeCo structures [12]), V_{in} — the input voltage, $\kappa = -2g_p g_m^{(3)} B/MH_A$, $\eta = -(g_m^{(1)} - 2g_m^{(2)})2B/MH_A$, $g_m^{(3)} = -14$ V, τ and τ_1 — charge relaxation times in the piezoelectric and dielectric layers, respectively. Ratio $2B/MH_A = -3 \cdot 10^3$ was used in calculations.

With the same variables, normalized output voltage $U_{out} = 2V_{out}g_p B/MH_A$ is determined by the input voltage and the solutions of the system of equations (2) and (3):

$$U_{out} = U_{in} + P - \kappa \sin 2\varphi. \tag{4}$$

According to Eq. (3), stable equilibrium at zero input signal corresponds to equality $P_0 = \kappa \sin 2\varphi_0$ that relates the charge at the upper piezoelectric plate to the direction of magnetization.

The response of the structure to a random impact was modeled with respect to a bistable state of the magnetic system in magnetization field $H = 1.05H_A$ ($\varphi_0 = -0.43$) that is weaker than field $H = 1.18H_A$ of the spin-reorientation transition. The input was an equidistant sequence of pulses of a Gaussian shape with a duration of $2.8 \cdot 10^{-3}\,\tau$ and a random amplitude distributed uniformly either over the $0 < U_{in} < U_{max}$ interval or over $-U_{max} < U_{in} < U_{max}$. The pulse repetition period was set to $0.02\,\tau$.

Figure 2 presents the results of calculation of the output voltage and angular deviation of magnetization from the initial equilibrium position at $U_{max} = 0.0442$, which is close to threshold $U_{th} = 0.044$ of switching of the bistable magnetic system between equilibrium states. It is evident that when a pulse with an amplitude above the threshold level arrives in a random sequence, a reverse-polarity spike pulse is generated at the output electrode (Fig. 2, *a*). The magnetic system remains in a switched state throughout the duration of such a pulse and returns to the initial equilibrium afterwards (Fig. 2, *b*). The switching of heterostructure states is established by the simultaneous operation of piezoelectric and magnetostriction mechanisms. Pulsed deformation induced in the structure by an electric field applied to the piezoelectric produces an effective magnetostriction anisotropy field in the magnetic layer. When the magnetostriction field strength exceeds a threshold value, the bistable magnetic subsystem switches from one stable state to another. The switching process is, in turn, accompanied by the generation of non-equilibrium magnetostriction stresses, which have a reverse effect on the piezoelectric layer, and induces an output voltage jump that is antiphase to the input voltage.

Note that the threshold value and the probability of switching are controlled by the magnetic field strength. Specifically, the threshold amplitude changes from $U_{th} = 0.049$ to $U_{th} = 0.039$ as the field strength increases from $H = 1.03H_A$ to $H = 1.07H_A$.

As supercriticality (i.e., the magnitude of U_{max} excess over threshold level $U_{th} = 0.044$) becomes more pronounced, the frequency of generation of spike pulses increases (Fig. 3, *a*); the amplitude virtually does not change from pulse to pulse, but the sequence of their generation becomes random,

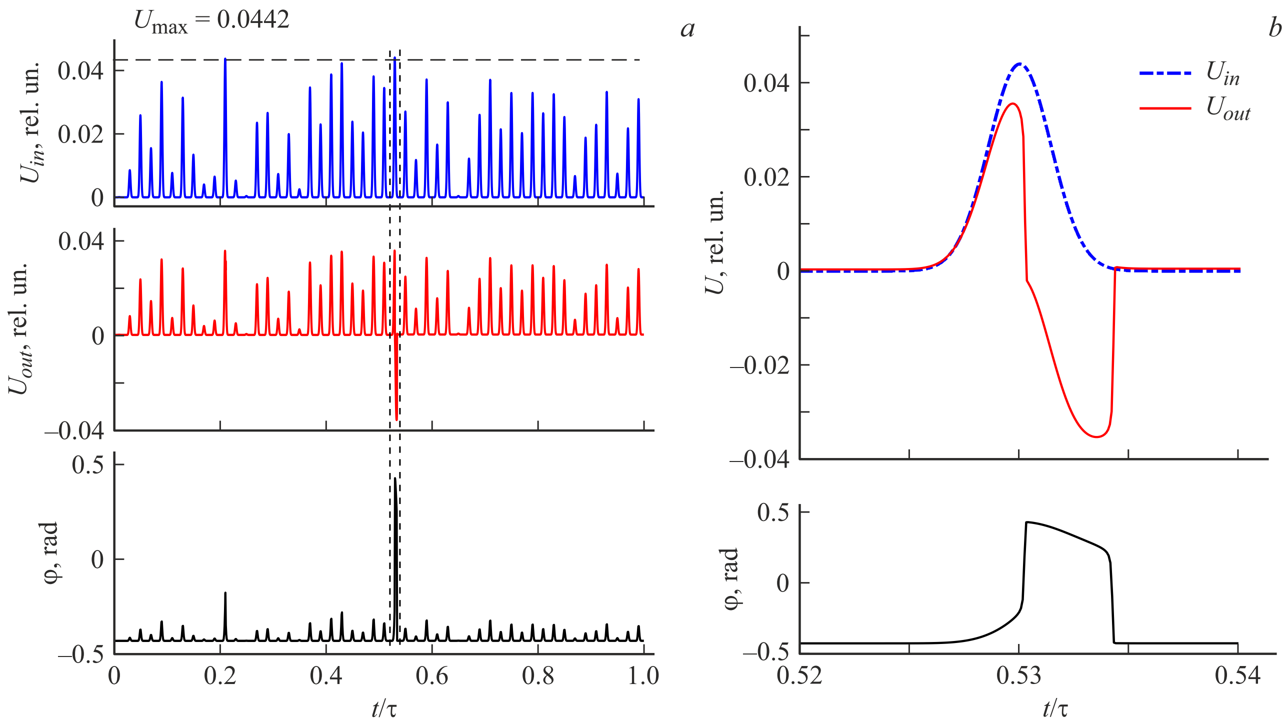

Figure 2. *a* — Diagrams of the random distribution of amplitudes of input pulse signals U_{in}, output signals U_{out}, and magnetization orientation angle φ under the conditions of generation of a single spike signal. The dashed line indicates the spike generation threshold. *b* — Shapes of the input pulse (dash-and-dot curve), the spike signal (solid curve), and the magnetization orientation angle. Dotted lines in panel *a* bound the region shown in detail in panel *b*.

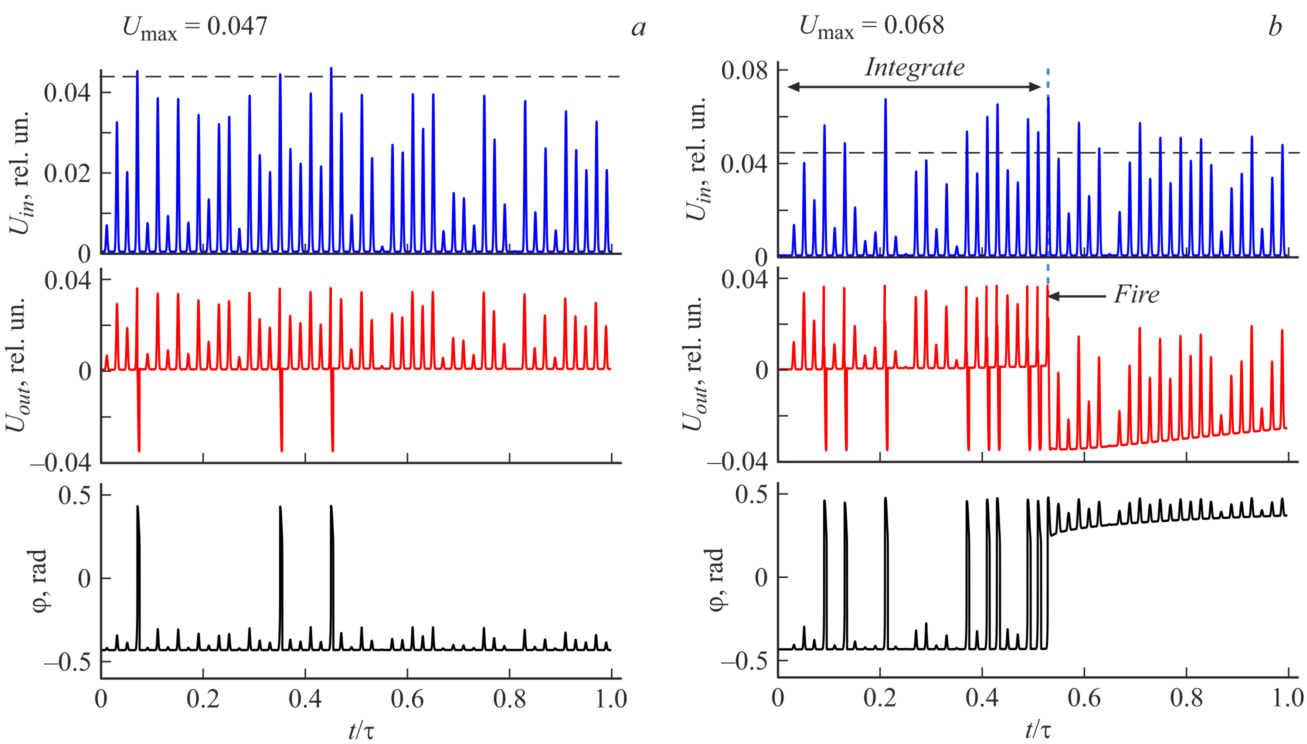

Figure 3. Diagrams of the distribution of amplitudes of input pulse signals U_{in}, output signals U_{out}, and magnetization orientation angle φ under the conditions of generation of a random sequence of spike signals (*a*) and in the mode of accumulation and threshold switching of the magnetization direction (*b*). The dashed line indicates the spike generation threshold.

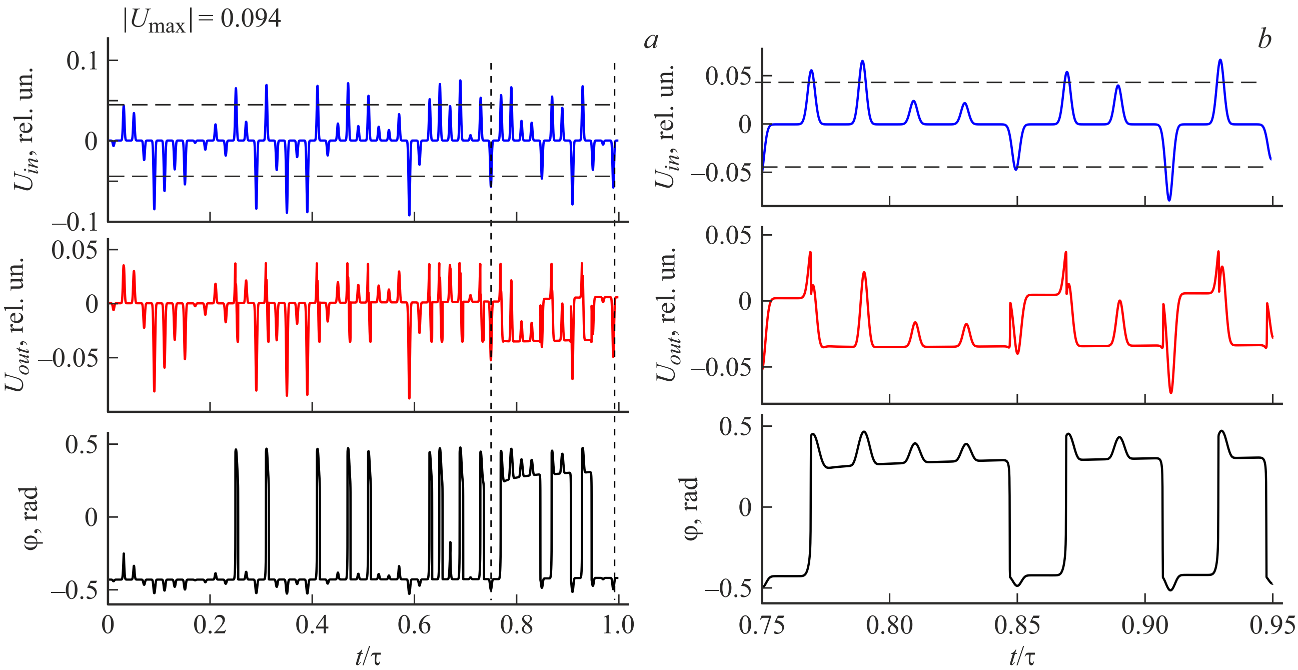

Figure 4. Diagrams of the distribution of amplitudes of input pulse signals U_{in}, output signals U_{out}, and magnetization orientation angle φ obtained when a bipolar random sequence of signals is fed to the cell input. *a* — Distributions within the time interval equal to charge relaxation time τ; *b* — fragment of the diagram in panel *a* within the time interval from 0.75τ to 0.95τ. Diagrams in panel *b* illustrate the random delay time of the magnetic subsystem in stable states. Dashed lines indicate the threshold levels of input signal amplitudes. Dotted lines in panel *a* bound the region shown in detail in panel *b*.

similar to a probabilistic bit (p-bit) [8,9]. With further growth of supercriticality, the effect of accumulation with a threshold transition of the magnetic system to a new stable state (integrate-and-fire) is manifested within the charge relaxation time (Fig. 3, *b*). The initial state is restored by applying a negative polarity pulse of a sufficient amplitude (reset pulse).

Pulse signals of different signs are fed to the input of systems of bipolar artificial neurons [15]. When the magnetoelectric cell is exposed to a random sequence of bipolar pulses, the quasi-stable stochastic spike generation mode (Fig. 4, *a*) with a random duration of stable states of the magnetic subsystem (Fig. 4, *b*) is established in it. The randomness of time spent by the magnetic system in stable states is ensured by the fact that reverse switching occurs only when a reverse-polarity pulse with an amplitude above the threshold value arrives. The moment of arrival of such a pulse is random due to the amplitude stochasticity of input pulse sequences.

The presented results illustrate the capacity for functional transformation of random pulse signals that is characteristic of a composite magnetoelectric cell with a spin-reorientation transition. Specifically, the cell implements threshold transformation of signals with random amplitude into signals of the „random bit" type. The transformation threshold is controlled by an external magnetic field, which may be used to train neuromorphic systems. The inverse transformation with modified statistics may be implemented in layered networks of the restricted Boltzmann machine (RBM) type [16]. The obtained characteristics and the accumulation and switching effects are of interest for applications in stochastic neuromorphic systems.

Funding

This study was supported financially by grant No. 23-19-00849 from the Russian Science Foundation.

Conflict of interest

The authors declare that they have no conflict of interest.

References

[1] O. Deperlioglu, U. Kose, Comput. Electr. Eng., **37**, 392 (2011). DOI: 10.1016/j.compeleceng.2011.03.010

[2] Z. Li, X. Geng, J. Wang, F. Zhuge, Front. Neurosci., **15**, 717947 (2021). DOI: 10.3389/fnins.2021.717947

[3] L.M. Krutyansky, V.L. Preobrazhensky, Tech. Phys. Lett., **49** (8), 28 (2023). DOI: 10.61011/TPL.2023.08.56683.19594.

[4] W. Yi, K.K. Tsang, S.K. Lam, X. Bai, J.A. Crowell, E.A. Flores, Nat. Commun., **9** (1), 4661 (2018). DOI: 10.1038/s41467-018-07052-w

[5] H. Liu, T. Wu, X. Yan, J. Wu, N. Wang, Z. Du, H. Yang, B. Chen, Z. Zhang, F. Liu, W. Wu, J. Guo, H. Wang, Nano Lett., **21**, 3465 (2021). DOI: 10.1021/acs.nanolett.1c00108

[6] A.Y. Morozov, K.K Abgaryan, D.L. Reviznikov, Nanotechnol. Russ., **16**, 767 (2021). DOI: 10.1134/S263516762106015X.
[7] J.J. Wang, S.G. Hu, X.T. Zhan, Q. Yu, Z. Liu, T.P. Chen, Y. Yin, S. Hosaka, Y. Liu, Sci. Rep., **8**, 12546 (2018). DOI: 10.1038/s41598-018-30768-0
[8] W.A. Borders, A.Z. Pervaiz, S. Fukami, K.Y. Camsari, H. Ohno, S. Datta, Nature, **573**, 390 (2019). DOI: 10.1038/s41586-019-1557-9
[9] J. Deng, V.P.K. Miriyala, Z. Zhu, X. Fong, G. Liang, IEEE Electron Dev. Lett., **41** (7), 1102 (2020). DOI: 10.1109/led.2020.2995874
[10] I. Chakraborty, G. Saha, A. Sengupta, K. Roy, Sci. Rep., **8**, 12980 (2018). DOI: 10.1038/s41598-018-31365-x
[11] F. Wang, L. Luo, D. Zhou, X. Zhao, H. Luo, Appl. Phys. Lett., **90**, 212903 (2007). DOI: 10.1063/1.2743393
[12] N. Tiercelin, V. Preobrazhensky, P. Pernod, Appl. Phys. Lett., **92**, 062904 (2008). DOI: 10.1063/1.2841656
[13] Y. Dusch, N. Tiercelin, A. Klimov, S. Giordano, V. Preobrazhensky, P. Pernod, J. Appl. Phys., **113**, 17C719 (2013). DOI: 10.1063/1.4795440
[14] A. Mazzamurro, Y. Dusch, P. Pernod, O. Bou Matar, A. Addad, A. Talbi, N. Tiercelin, Phys. Rev. Appl., **13**, 044001 (2020). DOI: 10.1103/PhysRevApplied.13.044001
[15] T. Kim, S.-H. Kim, J.-H. Park, J. Park, E. Park, S.-G. Kim, H.-Y. Yu, Adv. Electron. Mater., **7** (1), 2000410 (2020). DOI: 10.1002/aelm.202000410
[16] A. Fischer, C. Igel, Pattern Recogn., **47**, 25 2014). DOI: 10.1016/j.patcog.2013.05.025

Translated by D.Safin